

## Fabrication and characterization of $\text{Pb}_{1-x}\text{Yb}_x\text{Se}_{0.2}\text{Te}_{0.8}$ based alloy thin films thermoelectric generators grown using thermal evaporation method

Arshad Hmood<sup>a,1,2</sup>, Arej Kadhim<sup>b,1,2</sup>, Haslan Abu Hassan<sup>c,1</sup>

<sup>1</sup>Nano-Optoelectronic Research and Technology Laboratory (N.O.R.), School of Physics, Universiti Sains Malaysia, 11800 USM, Penang, Malaysia

<sup>2</sup>Department of Physics, College of Science, University of Basrah, Basrah, Iraq

<sup>a</sup>arshad.phy73@gmail.com, <sup>b</sup>arejkadhim@yahoo.com, <sup>c</sup>haslan@usm.my.

**Keywords:** Thermoelectric materials, thin films, thermoelectric devices.

**Abstract.** In the current work p- $\text{Pb}_{0.925}\text{Yb}_{0.075}\text{Te}:\text{Te}$  and n- $\text{Pb}_{0.925}\text{Yb}_{0.075}\text{Se}_{0.2}\text{Te}_{0.8}$  powders synthesized by solid-state microwave route were used to fabricating thermally evaporated thin films. The micro-thermoelectric devices were composed of 20-pairs and 10-pairs p- $\text{Pb}_{0.925}\text{Yb}_{0.075}\text{Te}:\text{Te}$  and n- $\text{Pb}_{0.925}\text{Yb}_{0.075}\text{Se}_{0.2}\text{Te}_{0.8}$  thin films on glass substrates. Overall size of the thin films thermoelectric generators which consist of 20-pairs and 10-pairs of legs connected by aluminum electrodes were 23 mm×20 mm and 12 mm×10 mm, respectively. The 20-pairs p–n thermocouples in series device generated output maximum open-circuit voltage of 275.3 mV and a maximum output power up to 54.4 nW at temperature difference  $\Delta T = 162$  K, and 109.4 mV and 16.7 nW at  $\Delta T=162$  K, for 10-pairs, respectively.

### Introduction

Interest in local cooling and low-power energy-scavenging applications has grown in the last decade. These applications have been used to generate a few microwatts of power at relatively high voltage to power small electronic devices, wireless sensors, wearable electronics, and other industrial heat-generating processes [1, 2]. However, recent significant advances in the scientific understanding of quantum well and nanostructure effects on TE properties and modern thin layer and nano-scale manufacturing technologies have combined to create the opportunity of advanced TE materials with potential conversion efficiencies of over 15% [3]. The advent of these advanced TE materials offers new opportunities to recover waste heat more efficiently and economically with highly reliable and relatively passive systems that produce no noise and vibration [4, 5]. A thermoelectric power generation (TEG) device produces voltage between the hot and the cold sides when a temperature difference ( $\Delta T$ ) between the two sides is present as a result of thermoelectric effect (TE). TE includes Seebeck (S), Peltier, and Thomson effects. TE is also associated with other effects such as Joulean and Fourier effects [6, 7]. TE generations have primarily focused on increasing the material figure of merit (ZT), which is the standard measure of a material's TE performance, and defined as  $ZT = S^2\sigma T/\kappa$ , where S is the Seebeck coefficient,  $\sigma$  the electrical conductivity,  $\kappa$  the thermal conductivity, and T is the absolute temperature. The product  $S^2\sigma$  is defined as the thermoelectric power factor [8]. The power factor should be maximized and the thermal conductivity should be minimized in order to achieve high efficiency thermoelectric materials. Recently developments in micro-thermoelectric devices used thin film depositions which are based on different growth methods such as molecular beam epitaxy (MBE) [9], electrochemical deposition [10], RF co-sputtering [5, 11], a simple vacuum thermal evaporation [6], flash evaporation [2], and co-evaporation [4], to grow single layers and super-lattices on various substrates [12]. We prepare  $\text{Pb}_{0.925}\text{Yb}_{0.075}\text{Te}:\text{Te}$  as p-type ingot and  $\text{Pb}_{0.925}\text{Yb}_{0.075}\text{Se}_{0.2}\text{Te}_{0.8}$  as n-type ingot using solid-state microwave for the fabrication of 20-pairs and 10-pairs of the thin films thermoelectric micro-devices (23mm × 20mm and 12mm × 10 mm, respectively) by a thermal evaporation method onto glass substrates. We investigate the intrinsic properties of each of the constituent thin films, and then we measure the output voltage and estimate the maximum output power of a complete generator in the temperature range of 298 K to 523 K as functions of the temperature difference between hot and cold junctions.

## Experimental

The n-type  $\text{Pb}_{0.925}\text{Yb}_{0.075}\text{Se}_{0.2}\text{Te}_{0.8}$  was synthesized as a quaternary compound by standard solid-state microwave route. Weighted 2 g amounts, according to the stoichiometric ratio  $\text{Pb}_{1-x}\text{Yb}_x\text{Se}_y\text{Te}_{1-y}$  ( $x=0.075$ ), and  $y=0.2$ . A typical element ratio for the preparation of  $\text{Pb}_{0.925}\text{Yb}_{0.075}\text{Se}_{0.2}\text{Te}_{0.8}$  is as follows: (1.1885 g) Pb, (0.0805 g) Yb, (0.0980 g) Se, and (0.6330 g) Te, were prepared from four high-purity element powders (Pb, Se, Te  $\geq 99.999\%$  100 meshes, and Yb  $\geq 99.9\%$  157  $\mu\text{m}$ ) as described elsewhere [13]. The polycrystalline alloys p-type of  $\text{Pb}_{0.925}\text{Yb}_{0.075}\text{Te}:\text{Te}$  was prepared by the same methods after the addition of excess Te. The thin films thermoelectric generators were then deposited onto clean glass substrates by thermal evaporation of  $10^{-6}$  mbar at room temperature using silicon monoxide (SM) boat design series SO-20 by (R. D. Mathis Co. USA). The p-type ( $\text{Pb}_{0.925}\text{Yb}_{0.075}\text{Te}:\text{Te}$ ) and n-type ( $\text{Pb}_{0.925}\text{Yb}_{0.075}\text{Se}_{0.2}\text{Te}_{0.8}$ ) powder were positioned in the load cavity of the boat, and when heated the vapors follow an indirect path through a series of baffles and then out the vertical chimney, of height and diameter measuring 12 mm and 6.3 mm, respectively. So the substrates do not see the bulk  $\text{Pb}_{1-x}\text{Yb}_x\text{Te}$  material at any time and this essentially eliminates any chance of spitting and streaming, which causes pinholes as shown in Fig. 1. The distance between the tantalum boat and the substrate is 180 mm.

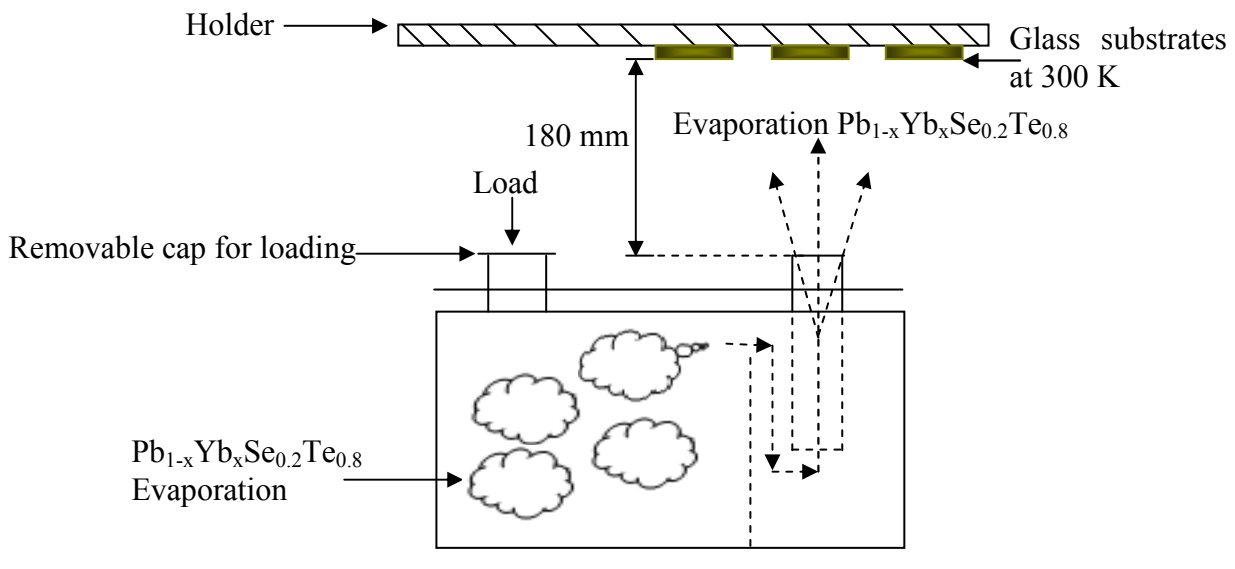


Fig.1: Scheme of SM boat used to prepare polycrystalline superlattice  $\text{Pb}_{1-x}\text{Yb}_x\text{Se}_{0.2}\text{Te}_{0.8}$  thin films.

The thicknesses of the thin films were determined to be approximately  $0.947 \mu\text{m}$  using an optical reflectometer (Filmatric F20, USA) measurement system. The patterned shadow masks fabricated 20-pairs and 10-pairs thermoelectric micro-devices ( $23 \text{ mm} \times 20 \text{ mm}$  and  $12 \text{ mm} \times 10 \text{ mm}$ , respectively) for the p and n-legs thin films and their junctions. Rectangular tracks on glass substrates had  $400 \mu\text{m}$  in width and  $20 \text{ mm}$  in length, for 20-pairs and rectangular ones –  $400 \mu\text{m}$  and  $10 \text{ mm}$  for 10-pairs, respectively (Fig.2(b)). The dimension of p- and n-legs was  $20 \text{ mm}$  or ( $10 \text{ mm}$ ) ( $l$ )  $\times$   $400 \mu\text{m}$  ( $w$ )  $\times$   $0.947 \mu\text{m}$  ( $t$ ), and the spacing between both legs was arranged to be  $150 \mu\text{m}$  are shown in Fig. 2. A diffusion barrier layer (Al-electrode) was also deposited between p- and n-type thin films thermoelectric generator at the junctions. The fundamental physical parameters of the semi-magnetic semiconductor lead chalcogenide thin films such as lattice constant, electrical conductivity, and the Seebeck coefficient are referred to in our previous papers [13]. We first measured the output voltage of the thin film thermoelectric generators while imposing a temperature gradient  $\Delta T = T_h - T_c$  between hot and cold junctions of the generators. The output voltage ( $V_{\text{out}}$ ), and the respective current, ( $I_{\text{out}}$ ) were measured at the Al-electrode pads connected to the thermoelectric legs. Measurement pairs of the voltage and current were acquired while the load

resistance,  $R_{Load}$  was manually adjusted. We also measured the internal resistance of the thin film thermoelectric generators by a two-wire method. The internal resistance, ( $R_{in}$ ) is modified by the contact resistances leading to  $R_{in} = R_{in-ideal} + R_{contact}$ , of the thermoelectric generator was calculated as follows:  $R_{in} = V_{oc}/I_{sc}$ , where  $V_{oc}$  is the open-circuit voltage and  $I_{sc}$  is the short-circuit current. The maximum output power of the thin film thermoelectric generators was estimated from the output voltage and the overall resistance of the generators.

## Results and discussion

The fabricated micro-device of p-Pb<sub>0.925</sub>Yb<sub>0.075</sub>Te:Te and n-Pb<sub>0.925</sub>Yb<sub>0.075</sub>Se<sub>0.2</sub>Te<sub>0.8</sub> thin films are shown in Fig. 2. Seen from the top view (SEM image of Fig. 2 (a)), the films are dense and uniform. The performance of lead–ytterbium–telluride films-based micro-generators is investigated at temperature range of 298-532 K. A temperature difference  $\Delta T$  was induced between the hot and cold junctions of the micro-generators, we the output voltage measured versus the output current output characteristic of the thermoelectric generators, and the maximum output power estimated.

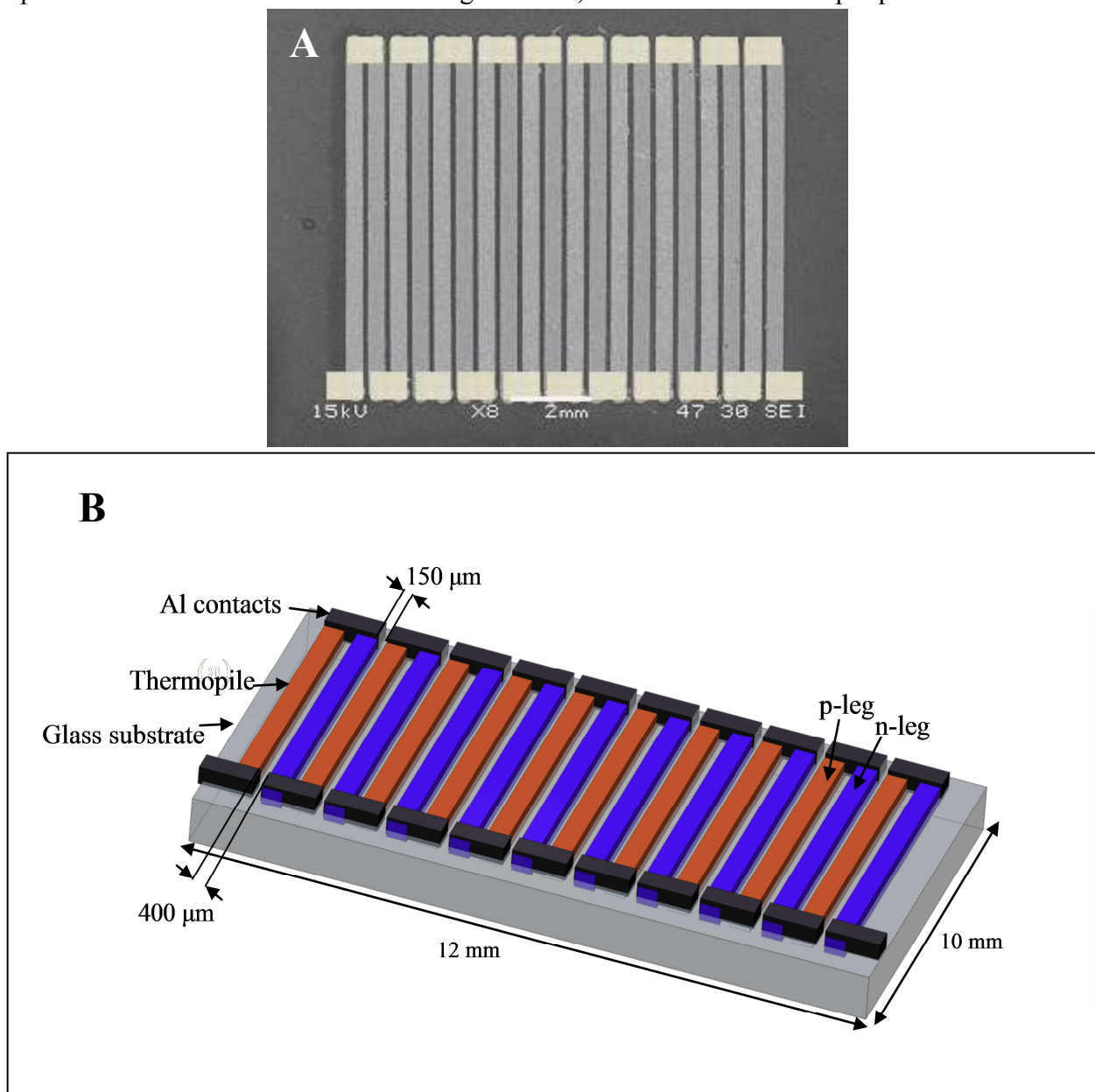
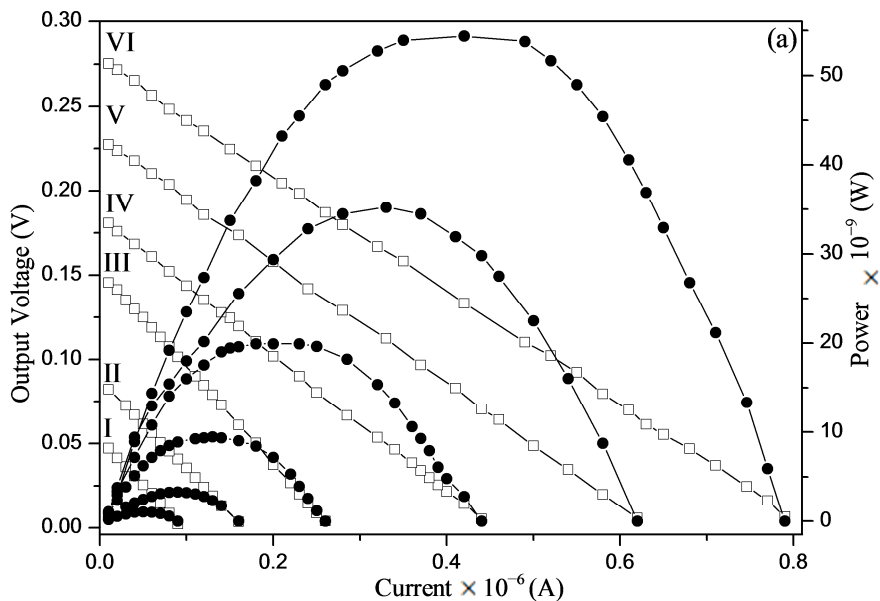


Fig.2: (a) SEM image of fabricated thin film thermoelectric generator on glass substrate, and (b) Schematic of thin film thermoelectric generator.

Fig. 3 shows the load characteristics of the two micro-generators, namely, the output voltage  $V_{out}$  dependences the output current  $I_{out}$  and output power  $P_{out}$  as functions of the temperature difference  $\Delta T$  for (a) 20-pairs and (b) 10-pairs micro-generators. As expected the output voltage increases with the temperature gradient,  $\Delta T$  increased, and this conclusion is valid for the plot of the Fig. 3 and for similar plots, since the gradient temperatures are such that the thermoelectric generators are not behind a certain thermal saturation point. It can be observed a high linearity in all  $V_{out}$  v.s  $I_{out}$  plots and almost the same slope. This means that the internal resistance  $R_{in}=V_{oc}/I_{sc}$  of the thermoelectric generators still constant with the gradient temperature and load resistance. From this analysis, it possible to conclude that the internal resistance of the analyzed thermoelectric devices are equal to  $R_{in} = 348 \text{ K}\Omega$  for 20-pairs, and  $179 \text{ K}\Omega$  for 10-pairs, respectively.

An analysis to both plots of the Figs. 3 (a) and (b) allows the observation of an increasing in the output power,  $P_{out}$ , with the temperatures gradient. Thus, the observation results from the rise of the temperature gradient,  $\Delta T$ , whose consequence is an increase in the output voltage,  $V_{out}$ . As this output voltage gets higher, the higher will be the output current  $I_{out}$  (considering several values for the load resistance) and therefore the higher will be the dissipated power in the external load resistance, e.g.  $P_{out} = R_{load}I_{out}^2$ . The alternative set of plots for the output power,  $P_{out}$ , versus the output current,  $I_{out}$  (or versus the load resistance,  $R_{load}$ ). Fig. 3 illustrates six plots for the six difference temperatures, an alternative set of plots, but for the output power,  $P_{out}$ , versus the output voltage,  $V_{out}$ . The voltage, or thermoelectric electromotive force (emf), produced by the Seebeck effect is defined as  $V_{out} = S_{p,n}\Delta T$ , where  $S_{p,n}$  indicates the relative Seebeck coefficient for a material pair p-n [11]. In order to maximize the generated output voltage, several thermocouples are connected electrically in series with each other and thermally in parallel to form a thermopile, which is able to generate  $n$  times the output voltage of one thermocouple (if  $n$  is the number of thermocouples in series) and a maximum output electric power (with optimal impedance matching) which can be expressed as  $P_{max} = \frac{(nS_{p,n}\Delta T)^2}{4R_{in}}$ , where  $R_{in}$  is the internal electrical resistance of the generator. The ideal internal electrical resistance is calculated from the thermocouple dimensions, the number of thermocouples in series, which is  $R_{in} = n (R_p+R_n)$  [14]. Assuming that the maximum output power is achieved when  $R_{load} = R_{in}$ , so the maximum output power of micro-generators estimated as functions of the temperature difference in this measured temperature region of  $\Delta T = 162 \text{ K}$  [15]. At the temperature difference of 162 K, the output voltage reaches 275.3 mV and 54.4 nW, respectively, for 20-pairs and 109.4 mV and 16.7 nW, respectively for 10-pairs.



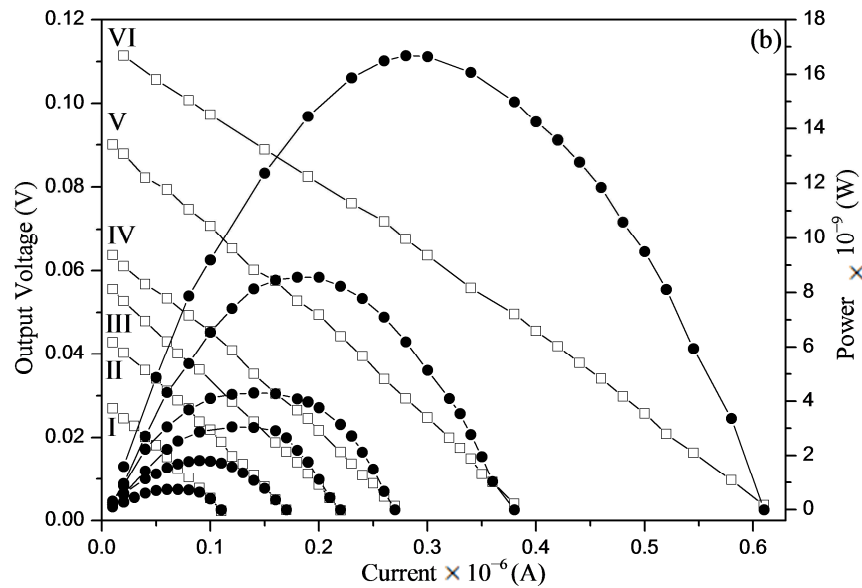


Fig. 3: Output power of the generator versus the output voltage and the output current of (a) 20-pair and (b) 10-pair thermoelectric devices with different temperature gradients  $\Delta T$  at (I)  $\Delta T=73$  K, (II)  $\Delta T=93$  K, (III)  $\Delta T=110$  K, (IV)  $\Delta T=121$  K, (V)  $\Delta T=141$  K, and (VI)  $\Delta T=162$  K.

In fact, the thermoelectric generators are generally based on Seebeck effect of heavily doped semiconductors to produce electrical energy [16-19]. In thermoelectric generator, another more appropriate performance factor is the power factor,  $S^2\sigma$  ( $\text{W}/\text{K}^2 \text{ m}^{-1}$ ). The  $S^2\sigma$  is defined as the electric power per unit area through which the heat flows, per unit temperature gradient between the hot and the cold sides [18]. This is attributed to the micro-structures not having been optimized and to the high contact resistance caused by the non-optimized bonding process [20]. It is well known that the electrical contact and thermal contact will play important roles in improving the device power-generation performance and related need contact problems to be minimized.

## Conclusion

The quaternary alloys films based micro-generators of micro-scale design have been successfully fabricated by a thermal evaporation method. We measured the performance of the micro-generators at 298–523 K. The high output voltages of 275.3 mV and 109.4 mV, and estimated output power of 54.4 nW and 16.7 nW, for 20-pairs and 10-pairs, respectively, have been obtained for a temperature difference  $\Delta T=162$  K. The low power generated by each device geometry means that these thermoelectric configurations are not get well enough adapted to supply high power but are interesting enough for temperature sensors due to their good sensitiveness in voltage. We can conclude that thermoelectric micro-devices exhibit scalability in output power per unit volume. The power values are low, mainly due to high electrical contact resistances of the chosen device geometry.

## Acknowledgments

The authors are grateful for the funding provided by the Postgraduate Research Grant Scheme (PRGS) (No.1001/PFIZIK/844134) of Universiti Sains Malaysia. We are also grateful for the Nano-Optoelectronics Research and Technology Laboratory (N.O.R.) of the School of Physics for the help extended during the research.

## References

- [1] M. Takashiri, T. Shirakawa, K. Miyazaki, H. Tsukamoto, Fabrication and characterization of bismuth–telluride-based alloy thin film thermoelectric generators by flash evaporation method, *Sens. Actuators A* 138 (2007) 329–334.
- [2] G. Savelli, M. Plissonnier, J. Bablet, C. Salvi, J.M. Fournier, Energy conversion using new thermoelectric generator, *MEMS/MOEMS - DTIP (2006)* ISBN: 2-916187-03-0.
- [3] Il-Ho Kim, (Bi,Sb)<sub>2</sub>(Te,Se)<sub>3</sub>-based thin film thermoelectric generators, *Mater. Lett.* 43 (2000) 221–224.
- [4] N. H. Bae, S. Han, K. E. Lee, B. Kim, S.-T. Kim, Diffusion at interfaces of micro thermoelectric devices, *Curr. Appl. Phys.* 11 (2011) S40–S44.
- [5] N. Kaiwa, M. Hoshino, T. Yaginuma, R. Izaki, S. Yamaguchi, A. Yamamoto, Thermoelectric properties and thermoelectric devices of free-standing GaN and epitaxial GaN layer, *Thin Solid Films* 515 (2007) 4501–4504.
- [6] M. Tan, Y. Wang, Y. Deng, Z. Zhang, B. Luo, J. Yang, Y. Xu, Oriented growth of A<sub>2</sub>Te<sub>3</sub> (A = Sb, Bi) films and their devices with enhanced thermoelectric performance, *Sens. Actuators A* 171 (2011) 252–259.
- [7] X. Niu, J. Yu, S. Wang, Experimental study on low-temperature waste heat thermoelectric generator, *J. Power Sou.* 188 (2009) 621–626.
- [8] D. Zhao, C. Tian, S. Tang, Y. Liu, L. Jiang, L. Chen, Fabrication of a CoSb<sub>3</sub>-based thermoelectric module, *Mater. Sci. Semicond. Process.* 13 (2010) 221–224.
- [9] G. Zeng, J. H. Bahk, J. E. Bowers, H. Lu, A. C. Gossard, S. L. Singer, A. Majumdar, Z. Bian, M. Zebarjadi, A. Shakouri, Thermoelectric power generator module of 16×16 Bi<sub>2</sub>Te<sub>3</sub> and 0.6% ErAs: (InGaAs)<sub>1-x</sub>(InAlAs)<sub>x</sub> segmented elements, *Appl. Phys. Lett.* 95 (2009) 083503.
- [10] W. Glatz, S. Muntwyler, C. Hierold, Optimization and fabrication of thick flexible polymer based micro thermoelectric generator, *Sens. Actuators A* 132 (2006) 337–345.
- [11] L. Francioso, C. De Pascali, I. Farella, C. Martucci, P. Cretì, P. Siciliano, Flexible thermoelectric generator for ambient assisted living wearable biometric sensors, *A. Perrone, J. Power Sou.* 196 (2011) 3239–3243.
- [12] R. Izaki, M. Hoshino, T. Yaginuma, N. Kaiwa, S. Yamaguchi, A. Yamamoto, Thermal properties and thermoelectric microdevices with InN thin films, *Microelectronics Journal* 38 (2007) 667–671.
- [13] A. Hmood, A. Kadhim, H. Abu Hassan, Composition-dependent structural and electrical properties of PbSe<sub>1-x</sub>Te<sub>x</sub> thin films, *Superlat. Microst.* 51 (2012) 825–833.
- [14] L. Han, Y. Jiang, S. Li, H. Su, X. Lan, K. Qin, T. Han, H. Zhong, L. Chen, D. Yu, High temperature thermoelectric properties and energy transfer devices of Ca<sub>3</sub>Co<sub>4-x</sub>Ag<sub>x</sub>O<sub>9</sub> and Ca<sub>1-y</sub>SmyMnO<sub>3</sub>, *J. Alloys Compd.* 509 (2011) 8970–8977.
- [15] S. M. Choi, K. H. Lee, C. H. Lim, W. S. Seo, Oxide-based thermoelectric power generation module using p-type Ca<sub>3</sub>Co<sub>4</sub>O<sub>9</sub> and n-type (ZnO)<sub>7</sub>In<sub>2</sub>O<sub>3</sub> legs, *Energy Conv. Manag.* 52 (2011) 335–339.
- [16] Y. Pei, A. D. La Londe, S. Iwanaga, G. J. Snyder, High thermoelectric figure of merit in heavy hole dominated PbTe, *Energy Environ. Sci.* 4 (2011) 2085–2089.
- [17] Yu. I. Ravich, S. A. Némov, Hopping Conduction via Strongly Localized Impurity States of Indium in PbTe and Its Solid Solutions, *Semiconductors* 36 (2002) 1–20.

- 
- [18] H. S. Dow, M. W. Oh, B. S. Kim, S. D. Park, B. K. Min, H. W. Lee, D. M. Weel, Effect of Ag or Sb addition on the thermoelectric properties of PbTe, *J. Appl. Phys.* 108 (2010) 113709.
- [19] H. Wang, Y. Pei, A. D. LaLonde, G. J. Snyder, Heavily doped p-type PbSe with high thermoelectric performance: an alternative for PbTe, *Adv. Mater.* 23 (2011) 1366–1370.
- [20] H.-B. Lee, H. J. Yang, J. H. We, K. Kim, K. C. Chol, B. J. Cho, Thin-film thermoelectric module for power generator applications using a screen-printing method, *J. Electron. Mater.* 40 (2011) 615-619.

**Fabrication and Characterization of  $\text{Pb}_{1-x}\text{Yb}_x\text{Se}_{0.2}\text{Te}_{0.8}$  Based Alloy Thin Films Thermoelectric Generators Grown Using Thermal Evaporation Method**

10.4028/www.scientific.net/MSF.756.259

**DOI References**

- [1] M. Takashiri, T. Shirakawa, K. Miyazaki, H. Tsukamoto, Fabrication and characterization of bismuth–telluride-based alloy thin film thermoelectric generators by flash evaporation method, *Sens. Actuators A* 138 (2007) 329–334.  
<http://dx.doi.org/10.1016/j.sna.2007.05.030>
- [3] Il-Ho Kim, (Bi, Sb)<sub>2</sub>(Te, Se)<sub>3</sub>-based thin film thermoelectric generators, *Mater. Lett.* 43 (2000) 221–224.  
[http://dx.doi.org/10.1016/S0167-577X\(99\)00239-6](http://dx.doi.org/10.1016/S0167-577X(99)00239-6)
- [5] N. Kaiwa, M. Hoshino, T. Yaginuma, R. Izaki, S. Yamaguchi, A. Yamamoto, Thermoelectric properties and thermoelectric devices of free-standing GaN and epitaxial GaN layer, *Thin Solid Films* 515 (2007) 4501–4504.  
<http://dx.doi.org/10.1016/j.tsf.2006.07.145>
- [6] M. Tan, Y. Wang, Y. Deng, Z. Zhang, B. Luo, J. Yang, Y. Xu, Oriented growth of A<sub>2</sub>Te<sub>3</sub> (A = Sb, Bi) films and their devices with enhanced thermoelectric performance, *Sens. Actuators A* 171 (2011) 252–259.  
<http://dx.doi.org/10.1016/j.sna.2011.09.020>
- [7] X. Niu, J. Yu, S. Wang, Experimental study on low-temperature waste heat thermoelectric generator, *J. Power Sou.* 188 (2009) 621–626.  
<http://dx.doi.org/10.1016/j.jpowsour.2008.12.067>
- [8] D. Zhao, C. Tian, S. Tang, Y. Liu, L. Jiang, L. Chen, Fabrication of a CoSb<sub>3</sub>-based thermoelectric module, *Mater. Sci. Semicond. Process.* 13 (2010) 221–224.  
<http://dx.doi.org/10.1016/j.mssp.2010.10.016>
- [10] W. Glatz, S. Muntwyler, C. Hierold, Optimization and fabrication of thick flexible polymer based micro thermoelectric generator, *Sens. Actuators A* 132 (2006) 337–345.  
<http://dx.doi.org/10.1016/j.sna.2006.04.024>
- [11] L. Francioso, C. De Pascali, I. Farella, C. Martucci, P. Creti, P. Siciliano, Flexible thermoelectric generator for ambient assisted living wearable biometric sensors, *A. Perrone, J. Power Sou.* 196 (2011) 3239–3243.  
<http://dx.doi.org/10.1016/j.jpowsour.2010.11.081>
- [12] R. Izaki, M. Hoshino, T. Yaginuma, N. Kaiwa, S. Yamaguchi, A. Yamamoto, Thermal properties and thermoelectric microdevices with InN thin films, *Microelectronics Journal* 38 (2007) 667–671.  
<http://dx.doi.org/10.1016/j.mejo.2007.05.005>
- [13] A. Hmood, A. Kadhim, H. Abu Hassan, Composition-dependent structural and electrical properties of PbSe<sub>1-x</sub>Te<sub>x</sub> thin films, *Superlat. Microst.* 51 (2012) 825–833.  
<http://dx.doi.org/10.1016/j.spmi.2012.04.001>
- [14] L. Han, Y. Jiang, S. Li, H. Su, X. Lan, K. Qin, T. Han, H. Zhong, L. Chen, D. Yu, High temperature thermoelectric properties and energy transfer devices of Ca<sub>3</sub>Co<sub>4-x</sub>Ag<sub>x</sub>O<sub>9</sub> and Ca<sub>1-y</sub>SmyMnO<sub>3</sub>, *J. Alloys Compd.* 509 (2011) 8970–8977.  
<http://dx.doi.org/10.1016/j.jallcom.2011.06.113>
- [15] S. M. Choi, K. H. Lee, C. H. Lim, W. S. Seo, Oxide-based thermoelectric power generation module

using p-type  $\text{Ca}_3\text{Co}_4\text{O}_9$  and n-type  $(\text{ZnO})_7\text{In}_2\text{O}_3$  legs, *Energy Conv. Manag.* 52 (2011) 335–339.

<http://dx.doi.org/10.1016/j.enconman.2010.07.005>

[16] Y. Pei, A. D. LaLonde, S. Iwanaga, G. J. Snyder, High thermoelectric figure of merit in heavy hole dominated PbTe, *Energy Environ. Sci.* 4 (2011) 2085–(2089).

<http://dx.doi.org/10.1039/c0ee00456a>

[17] Yu. I. Ravich, S. A. Némov, Hopping Conduction via Strongly Localized Impurity States of Indium in PbTe and Its Solid Solutions, *Semiconductors* 36 (2002) 1–20.

<http://dx.doi.org/10.1134/1.1434506>

[18] H. S. Dow, M. W. Oh, B. S. Kim, S. D. Park, B. K. Min, H. W. Lee, D. M. Wee, Effect of Ag or Sb addition on the thermoelectric properties of PbTe, *J. Appl. Phys.* 108 (2010) 113709.

<http://dx.doi.org/10.1063/1.3517088>

[19] H. Wang, Y. Pei, A. D. LaLonde, G. J. Snyder, Heavily doped p-type PbSe with high thermoelectric performance: an alternative for PbTe, *Adv. Mater.* 23 (2011) 1366–1370.

<http://dx.doi.org/10.1002/adma.201004200>

[20] H. -B. Lee, H. J. Yang, J. H. We, K. Kim, K. C. Chol, B. J. Cho, Thin-film thermoelectric module for power generator applications using a screen-printing method, *J. Electron. Mater.* 40 (2011) 615–619.

<http://dx.doi.org/10.1007/s11664-010-1481-0>